2023 62nd IEEE Conference on Decision and Control (CDC)
December 13-15, 2023. Marina Bay Sands, Singapore

Event-triggered Stabilization of Parabolic PDEs by Switching

Wen Kang, Emilia Fridman, Jing Zhang, Chuan-Xin Liu

***Abstract*— Although switching-based stabilization of 1D parabolic systems was investigated by employing one actuator moving in spatial domain in our recent paper [18], this method increases the system cost since actuator and sensor switching happens at fixed time regardless of whether the switching is necessary or not. To further reduce operating and production cost, in the present paper, switching-based dynamic event-triggered control law is studied to stabilize the parabolic PDE systems via output-dependent switching law. Constructive exponential stability conditions are established by using Lyapunov method. A numerical example shows the effectiveness of the proposed methods.**

I. INTRODUCTION

In recent years, event-triggered control is becoming a hot research area since it can reduce the amount of transmitted information and save the computation resources. Owing to the superior performance, some fruitful results on the event-triggered control of ODEs (see e.g. [1]-[3]) and PDEs (see e.g. [4]-[9]) have been reported. In general, the investigation on event-triggering mechanism (ETM) can be classified into two categories: dynamic ETM (see e.g. [1], [4]) and static ETM (see e.g. [2], [3], [6]). In [4], a dynamic event-triggered control law was proposed for a class of reaction-diffusion systems with Robin actuation. In [5], a static event-triggered controller was suggested for nonlinear Korteweg-de Vries equation.

A switching approach to ETM was introduced in [10] to reduce the amount of measurements to be sent. This new method has been applied for ODE systems, such as uncertain nonlinear systems in [11] and discrete-time switched systems in [12]. As for PDEs, the switching-based dynamic event-triggered control has been proposed in [13] for stabilizing a reaction-diffusion equation. Taking switching rule and ETM into account is of great importance for PDEs, which can further improve system performance.

The construction of switching rules for control of systems is an active research area. Due to its superior capability to reduce the energy, switching control law has been widely adopted for PDEs (see e.g. [14], [15], [16], [17]). In [14], [15], the implementation of optimal and switching policies of spatially scheduled actuators was created for a class of PDEs. In [16], [17], the integrated design of switching control and mobile actuator/sensor guidance was proposed to exponentially stabilize the reaction-diffusion equation. In our recent paper [18], a sampled-data switching-based controller was developed for 1D parabolic systems by employing one actuator moving in spatial domain. Although the sampled-data (time-triggered) switching control improves the performance with reduced operating and production costs, this method also increases the system cost since actuator switching happens at fixed time regardless of whether the switching is necessary or not. Therefore, the ETM was added into the switching rule to reduce the unnecessary switching cost and wear (see e.g. [19]-[22]), which has the advantage of reducing the frequency of transmissions and improving the utilization rate of system resources. Though some researchers have applied this novel scheme for PDEs to increase the utilization efficiency of the devices (see e.g. [21]) and save the computation resources (see e.g. [22]), it is worth to mention that the switching-based event-triggered control may be inefficient for the case of unstabilizable open-loop system, which motivates our study.

To further reduce the number of switches, in this paper, we focus on a switching-based event-triggered control strategy design for parabolic PDEs for the first time. The main contributions and challenges are summarized as follows:

- Compared with our previous result on switching control in [18], an improved scheme is considered by adding ETM to reduce the number of switches. A novel switching-based event-triggered controller is proposed for reaction-diffusion equation. The key idea of control strategy is to stabilize the system by using only one actuator that moves in the spatial domain and a dynamic ETM is designed to reduce the frequency of actuator switching (moving to another domain), thereby improving system performance.
- Different from the existing works on mobile actuators (see e.g. [14]-[17]), appropriate switching rule and ETM are proposed to stabilize the nonlinear reaction-diffusion equation by moving actuators. The guidance of active actuators is provided by the output-dependent switching.

The rest of paper is organized as follows. The problem statement and switching-based event-triggered control design are discussed in Section II. Section III is devoted to well-posedness and stability analysis. A numerical simulation is presented in Section IV. Finally, concluding remarks are given in Section V.

*This work was supported by National Natural Science Foundation of China (Grant No.62273046), Guangdong Basic and Applied Basic Research (Grant No. 2022A1515010039), Israel Science Foundation (Grant No. 673/19), Beijing Nova Program, and Beijing Institute of Technology Research Fund Program for Young Scholars (Grant No. 3170012222207).

Wen Kang and Jing Zhang are with School of Mathematics and Statistics, MIIT Key Laboratory of Mathematical Theory and Computation in Information Security, Beijing Institute of Technology, China (kangwen@amss.ac.cn; janet_zhangjing@163.com)

Emilia Fridman is with School of Electrical Engineering, Tel Aviv University, Israel (emilia@tauex.tau.ac.il)

Chuan-Xin Liu is with School of Automation and Electrical Engineering, University of Science and Technology Beijing, China (s20200565@xs.ustb.edu)

Notation. The symbol $*$ represents symmetric elements. The support of a function g is denoted by supp$g$, and conv(supp$g$) represents the convex hull of supp$g$. $L^2(0,L)$ stands for the Hilbert space of square integrable scalar functions $f(x)$ on $(0,L)$ with the corresponding norm $\|f\|_{L^2(0,L)} = [\int_0^L f^2(x)dx]^{\frac{1}{2}}$. $L^\infty(0,L)$ denotes the space of essentially bounded function $f(x)$ on $(0,L)$ with he corresponding norm $\|f\|_{L^\infty(0,L)} = \operatorname*{ess\,sup}_{x\in[0,L]} |f(x)|$. The Sobolev space $H^k(0,L)$ with $k \in \mathbb{Z}$ is defined as $H^k(0,L) = \{f : f^{(\alpha)} \in L^2(0,L),\ \forall\ 0 \le |\alpha| \le k\}$ with norm $\|f\|_{H^k(0,L)} = \{\sum_{0\le|\alpha|\le k} \|f^{(\alpha)}\|^2_{L^2(0,L)}\}^{\frac{1}{2}}$. $H_0^k(0,L) = \{f \in H^k(0,L) | f(0) = f'(0) = ... = f^{(k-1)}(0) = 0, f(L) = f'(L) = ... = f^{(k-1)}(L) = 0\}$.

II. Problem Formulation

Let $0 = t_0 < t_1 < \ldots < t_k < t_{k+1} < \ldots,\ \lim_{k\to\infty} t_k = \infty$ be a sequence of sampling instants that will be determined by dynamic ETM later. Consider the following nonlinear reaction-diffusion PDE:

$$\begin{cases} z_t(x,t) = \frac{\partial}{\partial x}[a(x)z_x(x,t)] + \varphi(z(x,t)) + b_{\sigma_k}(x)u_{\sigma_k}(t), \\ \qquad\qquad x \in \Omega,\ t \in [t_k, t_{k+1}), \\ z(x,0) = z_0(x), \end{cases} \tag{2.1}$$

where $k \in \mathbb{Z}_+^0$, under the Dirichlet

$$z(0,t) = z(l,t) = 0,\ t > 0, \tag{2.2}$$

or Neumann boundary conditions

$$z_x(0,t) = z_x(l,t) = 0,\ t > 0, \tag{2.3}$$

where $\Omega = [0,l]$ stands for spatial domain, $z(x,t)$ is the state of reaction-diffusion equation, $z_0(x)$ is the initial state, $u_{\sigma_k}(t)$ is the control input of the plant. The switching function $\sigma_k : k \in \mathbb{Z}_+ \to \{1,\ldots,N\}$ selects at each sampling time t_k one of the N available actuators corresponding to the shape function $b_{\sigma_k}(x)$ that will be shortly defined. The unknown function $a(x)$ is of class C^1 such that $0 < a_0 < a(x)$ for $x \in \Omega$, where a^0 is known bound. We make the following assumptions:

- Nonlinearity: It is supposed that the nonlinear function φ is of class C^1 and satisfies the following inequality
$$\varphi^2(z(x,t)) \le \phi z^2(x,t), \tag{2.4}$$
where ϕ is some positive constant. The open-loop system (2.1) may become unstable if ϕ is large enough.
- Spatial sampling: Following [23], [24], we divide Ω into N equal-length subintervals $\Omega_j = [x_{j-1}, x_j)(j = 1,\ldots,N)$ with the points $0 = x_0 < x_1 < \cdots < x_N = l$. Therefore, the length of each interval is given by $|\Omega_j| = \frac{l}{N}$. The shape functions $b_j(x)$ are chosen to be characteristic functions $b_j(x)$ of Ω_j as follows:
$$\begin{cases} b_j(x) = 0,\ x \notin \Omega_j, \\ b_j(x) = 1,\ \textit{otherwise}, \end{cases} \quad j = 1,\ldots,N. \tag{2.5}$$
- Measurements: Assume that N sensors provide the averaged state measurements:
$$y_j(t) = \frac{\int_{\Omega_j} z(x,t)dx}{|\Omega_j|} = \frac{N}{l}\int_{\Omega_j} z(x,t)dx \tag{2.6}$$
- Switching rule: Define the following switching law [18]:
$$\sigma_k = \arg\max_j \left[\int_{\Omega_j} z(x,t_k)dx\right]^2, \tag{2.7}$$
which means that the σ_k-th mode is active if
$$\left[\int_{\Omega_j} z(x,t_k)dx\right]^2 \le \left[\int_{\Omega_{\sigma_k}} z(x,t_k)dx\right]^2,\ \forall j = 1,\ldots,N. \tag{2.8}$$
- Moving time: The moving time $\delta \in (0,h_0)$ for actuators to the appropriate domain Ω_{σ_k} is taken into account similar to [18]. Therefore, the length of sampling subintervals in time satisfies $0 < h_0 \le t_{k+1} - t_k$.
- Time sampling: Inspired by [13], the sampling instants $0 = t_0 < t_1 < \ldots < t_k < t_{k+1} < \ldots,\ \lim_{k\to\infty} t_k = \infty$ is determined by the following dynamic ETM:
$$t_{k+1} = \min\{t > t_k + h_0 \,|\, |e_{\sigma_k}(t)|^2 - \varepsilon|y_{\sigma_k}(t)|^2 > \theta m(t)\} \tag{2.9}$$
where $\varepsilon > 0$, $\theta > 0$ and $e_j(t) = y_j(t) - y_j(t_k)$, $j = 1,2,\ldots,N$ are continuous in time. The dynamic variable $m(t)$ satisfies the following differential equation:
$$\dot{m}(t) = \begin{cases} -2\varepsilon_1 m(t), & t \in [t_k, t_k + h_0), \\ -\varepsilon_0 m(t) + \varepsilon|y_{\sigma_k}(t)|^2 - |e_{\sigma_k}(t)|^2, & t \in [t_k + h_0, t_{k+1}), \end{cases}$$
for scalar parameters $\varepsilon_0 > 0$ and $\varepsilon_1 > 0$. Assume that the initial condition $m(0) = m_0 \ge 0$, which implies that $m(t) \ge 0$ for $t \in [0,\infty)$. This dynamic ETM can determine the sampling instants at which the measurements and the switching control law need to be updated, whereas the actuator starts moving to the resulting zone.

In order to take into account the moving time of actuators, we follow [18] and consider additional switching between the open-loop system (when the actuator is moving) during the part of the sampling interval and the closed-loop switched system during the remaining part of the interval. Then the switching-based dynamic event-triggered control law is presented as follows:

$$u_{\sigma_k}(t) = \begin{cases} 0, & t \in [t_k, t_k + \delta), \\ -Ky_{\sigma_k}(t_k), & t \in [t_k + \delta, t_{k+1}) \end{cases} \tag{2.10}$$

with some $K > 0$. The switching signal σ_k is calculated at time t_k, whereas it takes δ seconds for actuators to move to the domain Ω_{σ_k}. Define a characteristic function:

$$\chi_{[a,b]}(t) = \begin{cases} 1, & \text{if } t \in [a,b], \\ 0, & \text{otherwise.} \end{cases} \tag{2.11}$$

Then the closed-loop system can be presented as two switches between three systems. The first one (for $t \in [t_k, t_k + \delta)$) is governed by

$$\begin{aligned} z_t(x,t) = {} & \frac{\partial}{\partial x}[a(x)z_x(x,t)] + \varphi(z(x,t)) \\ & - \frac{KN}{l}\left[1 - \chi_{[t_k,t_k+\delta]}(t)\right] b_{\sigma_k}(x) \int_{\Omega_{\sigma_k}} z(x,t_k)dx. \end{aligned} \tag{2.12}$$

The second one (for $t \in [t_k + \delta, t_k + h_0)$) is governed by (2.12) where the ETM is not activated. The third one (for $t \in [t_k + h_0, t_{k+1})$) is governed by (2.12) subject to the continuous ETM (2.9).

III. MAIN RESULTS

In this section, the well-posedness of the controlled system will be analyzed. Furthermore, we will give the stability analysis of the system under the switching-based event-triggered controller.

A. Well-posedness of the controlled system

Now we employ the step method (see Section 1.2 in [26]) to analyze the well-posedness of the system.

For $t \in [t_0, t_1]$, we assume that the σ_k-th mode is active. The system (2.1) via the switching-based event-triggered controller under the Dirichlet boundary conditions (2.2) can be rewritten to the following equation:

$$\begin{cases} \dfrac{d}{dt} z(\cdot,t) = \mathscr{A} z(\cdot,t) + \mathscr{F}(z(\cdot,t)), \\ z(\cdot,0) = z_0(\cdot), \end{cases} \tag{3.1}$$

where dissipative operator $\mathscr{A} = \frac{\partial}{\partial x}[a(x)\frac{\partial}{\partial x}]$ has the dense domain

$$\mathscr{D}((-\mathscr{A})^{\frac{1}{2}}) = H_0^1(0,l) = \{f \in H^1(0,1) | f(0) = f(l) = 0\}$$

with the norm $\|f\|_{H_0^1(0,l)} = \|f'\|_{L^2(0,l)}$. The nonlinear term $\mathscr{F}$ is defined as follows:

$$\mathscr{F}(z(\cdot,t)) = \begin{cases} \varphi(z(\cdot,t)), t \in [t_0, t_0+\delta] \\ \varphi(z(\cdot,t)) - \frac{KN}{l} b_{\sigma_k}(x) \int_{\Omega_{\sigma_k}} z_0(x)dx, t \in [t_0+\delta, t_1]. \end{cases}$$

Note that $\mathscr{F}$ is locally Lipschitz continuous, Therefore, for $z_1, z_2 \in H_0^1(0,l)$ with $\|z_1\|_{H_0^1(0,l)} \leq C$, $\|z_2\|_{H_0^1(0,l)} \leq C$, we have

$$\|\mathscr{F}(z_1) - \mathscr{F}(z_2)\|_{L^2(0,l)} \leq \kappa(C,\phi)\|z_1 - z_2\|_{H_0^1(0,l)},$$

where $\kappa(C,\phi)$ is a positive constant. From Theorem 3.3.3 of [27], we have that there exists a unique strong solution on $[t_0, t_1]$ for any initial condition $z_0 \in H_0^1(0,l)$.

Then we continue the same procedure for $t \in [t_1, t_2]$, $t \in [t_2, t_3]$, ... Finally, step by step we conclude that the strong solution exists for all $t \geq 0$ in the sense that

$$\begin{aligned} &z \in C([0,\infty); H_0^1(0,l)) \cap L^2([0,\infty); \mathscr{D}(\mathscr{A})), \\ &\dot{z} \in L^2([0,\infty); L^2(0,l)). \end{aligned}$$

B. Stability analysis of the controlled system

Denote $f_j(x,t) \triangleq z(x,t) - \frac{\int_{\Omega_j} z(\xi,t)d\xi}{|\Omega_j|}$. The switching-based event-triggered control (2.10) can be rewritten as

$$u_{\sigma_k}(t) = \begin{cases} 0, & t \in [t_k, t_k+\delta), \\ -K[z(x,t) - e_{\sigma_k}(t) - f_{\sigma_k}(x,t)], & t \in [t_k+\delta, t_{k+1}). \end{cases} \tag{3.2}$$

whereas the switching law chooses σ_k that satisfies:

$$\begin{aligned} &\int_{\Omega_j} [z(x,t) - e_j(t) - f_j(x,t)]^2 dx \\ &\leq \int_{\Omega_{\sigma_k}} \left[z(x,t) - e_{\sigma_k}(t) - f_{\sigma_k}(t)\right]^2 dx, \ j = 1,2,\ldots,N. \end{aligned} \tag{3.3}$$

Therefore, the closed-loop system (2.12) has the form of

$$\begin{aligned} &z_t(x,t) = \tfrac{\partial}{\partial x}[a(x) z_x(x,t)] + \varphi(z(x,t)) \\ &-K(1 - \chi_{[t_k,t_k+\delta]}) b_{\sigma_k}(x)[z(x,t) - e_{\sigma_k}(t) - f_{\sigma_k}(x,t)] \end{aligned} \tag{3.4}$$

on $t \in [t_k, t_k+\delta)$. For $t \in [t_k+\delta, t_k+h_0)$, the closed-loop system is (3.4) where the ETM is not activated. For $t \in [t_k+h_0, t_{k+1})$ the closed-loop system is (3.4) subject to the continuous ETM (2.9).

To study the stability of (3.4), we suggest the following switching Lyapunov functional:

$$V(t) = V_{P_1}(t) + V_{P_2}(t) + \chi_{[t_k+\delta, t_k+h_0]}(t) V_R(t) + m(t) \tag{3.5}$$

where $t \in [t_k, t_{k+1})$ and

$$\begin{aligned} &V_{P_1}(t) = P_1 \int_0^l z^2(x,t)dx, \\ &V_{P_2}(t) = P_2 \int_0^l a(x) z_x^2(x,t)dx, \\ &V_R(t) = R(h_0 + t_k - t) \int_0^l \int_{t_k+\delta}^t e^{-2\alpha(t-s)} z_s^2(x,s)dsdx. \end{aligned} \tag{3.6}$$

Note that $m(t) \geq 0$ implies that $V(t)$ is positive definite. To choose h_0 suitably, inspired by [24] and [26], we use a functional $V_R(t)$ to calculate the maximal value of h_0. From (3.6), it follows that $V_R(t_k+\delta) = V_R(t_k+h_0) = 0$, which implies that $V(t)$ is a continuous function for $t \in [0,\infty)$.

Theorem 3.1: Consider the closed-loop system (3.4) subject to Dirichlet boundary conditions (2.2). Given positive parameters K, h_0, θ, ε_0, ε, α, δ, $\varepsilon_1 > \alpha$, $h_0 > \delta$ and tuning parameter α_0 such that $\alpha h_0 > (\alpha_0 + \alpha)\delta$, let there exist scalars $P_n \geq 0$ $(n = 1,2,3,4)$, $\lambda_i \geq 0$ $(i = 0,1,2,3,4)$ and $R \geq 0$ that satisfy the LMIs:

$$2\alpha a_0 P_2 - 2a_0 P_4 + \frac{\lambda_2 l^2}{N^2\pi^2} + \frac{\lambda_3 l^2}{\pi^2} < 0 \tag{3.7}$$

$$2\alpha + \frac{l}{N}\lambda_4\theta - \varepsilon_0 < 0, \tag{3.8}$$

$$\Psi_m < 0, \ m = 0,1,2, \tag{3.9}$$

where

$$\Psi_0 = \begin{bmatrix} -2\alpha_0(P_1 + P_2 a_0 \frac{\pi^2}{l^2}) + \lambda_0\phi & P_1 - P_3 & P_3 \\ * & -2P_2 & P_2 \\ * & * & -\lambda_0 \end{bmatrix}, \tag{3.10}$$

$$\Psi_1 = \begin{bmatrix} \Psi_{11}^1 & \Psi_{12}^1 & P_4 & \frac{\lambda_1}{N-1} & \frac{\lambda_1}{N-1} \\ * & \Psi_{22}^1 & P_2 & 0 & 0 \\ * & * & -\lambda_0 & 0 & 0 \\ * & * & * & \Psi_{44}^1 & -\frac{\lambda_1}{N-1} \\ * & * & * & * & \Psi_{55}^1 \end{bmatrix}, \tag{3.11}$$

$$\Psi_2 = \begin{bmatrix} \Psi_{11}^2 & \Psi_{12}^2 & P_4 & P_4K - \lambda_1 & P_4K - \lambda_1 \\ * & \Psi_{22}^2 & P_2 & P_2K & P_2K \\ * & * & -\lambda_0 & 0 & 0 \\ * & * & * & \Psi_{44}^2 & \lambda_1 \\ * & * & * & * & \Psi_{55}^2 \end{bmatrix}, \tag{3.12}$$

$$\Psi_3 = \begin{bmatrix} \Psi_{11}^3 & \Psi_{12}^3 & P_4 & \frac{\lambda_1}{N-1} & \frac{\lambda_1}{N-1} \\ * & -2P_2 & P_2 & 0 & 0 \\ * & * & -\lambda_0 & 0 & 0 \\ * & * & * & \Psi_{44}^3 & -\frac{\lambda_1}{N-1} \\ * & * & * & * & \Psi_{55}^3 \end{bmatrix}, \tag{3.13}$$

$$\Psi_4 = \begin{bmatrix} \Psi_{11}^4 & \Psi_{12}^4 & P_4 & P_4K-\lambda_1 & P_4K-\lambda_1 \\ * & -2P_2 & P_2 & P_2K & P_2K \\ * & * & -\lambda_0 & 0 & 0 \\ * & * & * & \Psi_{44}^4 & \lambda_1 \\ * & * & * & * & \Psi_{55}^4 \end{bmatrix}, \tag{3.14}$$

$\Psi_{11}^1 = \Psi_{11}^3 = 2\alpha P_1 + \lambda_0\phi - \lambda_3 - \frac{\lambda_1}{N-1}$, $\Psi_{12}^1 = \Psi_{12}^3 = P_1 - P_4$,
$\Psi_{22}^1 = \Psi_{22}^2 = R(h_0-\delta) - 2P_2$, $\Psi_{44}^1 = \Psi_{44}^3 = -\frac{\lambda_1}{N-1} - \lambda_2$,
$\Psi_{55}^1 = -\frac{\lambda_1}{N-1} - \frac{Re^{-2\alpha(h_0-\delta)}}{h_0-\delta}$,
$\Psi_{11}^2 = 2\alpha P_1 + \lambda_0\phi - \lambda_3 + \lambda_1 - 2KP_4$, $\Psi_{12}^2 = \Psi_{12}^4 = P_1 - P_4 - KP_2$,
$\Psi_{44}^2 = \Psi_{44}^4 = \lambda_1 - \lambda_2$, $\Psi_{55}^2 = \lambda_1 - \frac{Re^{-2\alpha(h_0-\delta)}}{h_0-\delta}$, $\Psi_{55}^3 = -\frac{\lambda_1}{N-1}$,
$\Psi_{11}^4 = 2\alpha P_1 + \lambda_0\phi - \lambda_3 + \lambda_1 - 2KP_4 + \lambda_4\varepsilon + \frac{N\varepsilon}{l}$,
$\Psi_{55}^4 = \lambda_1 - \lambda_4 - \frac{N}{l}$.

Let α_1 be subject to

$$0 < \alpha_1 h_0 < \alpha h_0 - (\alpha_0 + \alpha)\delta. \tag{3.15}$$

Then the closed-loop system (2.12) subject to (2.2) and (2.7) is asymptotically stable for any initial function $z_0 \in H_0^1(0,l)$.

Proof: **Step 1:** For $t \in [t_k, t_k+\delta)$, the ETM is not activated. Therefore, we derive sufficient LMI-based conditions to guarantee that $\dot V(t) - 2\alpha_0 V(t) \le 0$.

Differentiating Lyapunov functional (3.5) along (3.4), we have

$$\begin{aligned}\dot V_{P_1}(t) - 2\alpha_0 V_{P_1}(t) &= 2P_1 \textstyle\int_0^l z_t(x,t)z(x,t)dx \\ &\quad -2\alpha_0 P_1 \textstyle\int_0^l z^2(x,t)dx,\end{aligned} \tag{3.16}$$

$$\begin{aligned}\dot V_{P_2}(t) - 2\alpha_0 V_{P_2}(t) &= 2P_2 \textstyle\int_0^l a(x) z_{xt}(x,t) z_x(x,t)dx \\ &\quad -2\alpha_0 P_2 \textstyle\int_0^l a(x) z_x^2(x,t)dx,\end{aligned} \tag{3.17}$$

$$\dot m(t) - 2\alpha_0 m(t) = -2(\varepsilon_1 + \alpha_0) m(t) \le 0. \tag{3.18}$$

From (2.4) we have

$$\lambda_0 \int_0^l [\phi z^2(x,t) - \varphi^2(z(x,t))]dx \ge 0. \tag{3.19}$$

Wirtinger's inequality yields

$$-2\alpha_0 P_2 \int_0^l a(x) z_x^2(x,t)dx \le -2\alpha_0 P_2 a_0 \frac{\pi^2}{l^2} \int_0^l z^2(x,t)dx,$$

We apply further the descriptor method [26] to (3.4), where the left-hand side of the following equation

$$2\textstyle\int_0^l [P_3 z(x,t) + P_2 z_t(x,t)]\Big[-z_t(x,t) + \frac{\partial}{\partial x}[a(x)z_x(x,t)] + \varphi(z(x,t))\Big]dx = 0$$

with some $P_3 > 0$ is added to $\dot V$.

Set $\eta_0 = \mathrm{col}\{z(x,t), z_t(x,t), \varphi(z(x,t))\}$. Therefore, we have

$$\dot V(t) - 2\alpha_0 V(t) \le \textstyle\int_0^l \eta_0^T \Psi_0 \eta_0 dx \le 0, \ t \in [t_k, t_k+\delta),$$

if $\Psi_0 \le 0$ holds.

Step 2: For $t \in [t_k+\delta, t_k+h_0)$, the ETM is not activated. To obtain the maximal value of the waiting time, we derive sufficient conditions to guarantee that $\dot V(t) + 2\alpha V(t) \le 0$.

Differentiating (3.5) along (3.4), we have

$$\begin{aligned}\dot V_{P_1}(t) + 2\alpha V_{P_1}(t) &= 2P \textstyle\int_0^l z_t(x,t)z(x,t)dx \\ &\quad +2\alpha P_1 \textstyle\int_0^l z^2(x,t)dx,\end{aligned} \tag{3.20}$$

$$\begin{aligned}\dot V_{P_2}(t) + 2\alpha V_{P_2}(t) &= 2P_2 \textstyle\int_0^l a(x) z_{xt}(x,t) z_x(x,t)dx \\ &\quad +2\alpha P_2 \textstyle\int_0^l a(x) z_x^2(x,t)dx,\end{aligned} \tag{3.21}$$

$$\begin{aligned}\dot V_R(t) + 2\alpha V_R(t) &= R(h_0 + t_k - t)\textstyle\int_0^l z_t^2(x,t)dx \\ &\quad -R\textstyle\int_0^l \int_{t_k+\delta}^t e^{-2\alpha(t-s)} z_s^2(x,s)dsdx,\end{aligned} \tag{3.22}$$

$$\dot m(t) + 2\alpha m(t) = 2(\alpha - \varepsilon_1) m(t). \tag{3.23}$$

Jensen's inequality leads to

$$\begin{aligned}&-R\textstyle\int_0^l \int_{t_k+\delta}^t e^{-2\alpha(t-s)} z_s^2(x,s)dsdx \\ &\le \frac{-Re^{-2\alpha(h_0-\delta)}}{h_0-\delta} \textstyle\int_0^l [z(x,t) - z(x,t_k)]^2 dx \\ &= \frac{-Re^{-2\alpha(h_0-\delta)}}{h_0-\delta} \textstyle\sum_{j=1}^N \int_{\Omega_j} e_j^2(t)dx.\end{aligned} \tag{3.24}$$

Note that $|\Omega_j| = \frac{l}{N}$. Therefore, (3.3) implies

$$\begin{aligned}&-\tfrac{\lambda_1}{N-1}\sum_{j\ne\sigma_k}^{N} \textstyle\int_{\Omega_j} [z(x,t) - e_j(t) - f_j(x,t)]^2 dx \\ &+\lambda_1 \textstyle\int_{\Omega_{\sigma_k}} [z(x,t) - e_{\sigma_k}(t) - f_{\sigma_k}(x,t)]^2 dx \ge 0,\end{aligned} \tag{3.25}$$

where $\lambda_1 \ge 0$.

Since $\int_{\Omega_j} f_j(x,t)dx = 0$, Poincaré's inequality leads to

$$\frac{\lambda_2 l^2}{N^2\pi^2} \int_0^l z_x^2(x,t)dx - \lambda_2 \sum_{j=1}^N \int_{\Omega_j} f_j^2(x,t)dx \ge 0, \tag{3.26}$$

where $\lambda_2 \ge 0$. Furthermore, Wirtinger's inequality yields

$$\frac{\lambda_3 l^2}{\pi^2} \int_0^l z_x^2(x,t)dx - \lambda_3 \int_0^l z^2(x,t)dx \ge 0, \tag{3.27}$$

where $\lambda_3 \ge 0$.

We apply further the descriptor method [26] to (3.4), where the left-hand side of the following equation

$$\begin{aligned}&2\textstyle\int_0^l [P_4 z(x,t) + P_2 z_t(x,t)]\Big[-z_t(x,t) + \frac{\partial}{\partial x}[a(x)z_x(x,t)] \\ &+\varphi(z(x,t),x,t) - Kb_{\sigma_k}(x)[z(x,t) - e_{\sigma_k}(t) - f_{\sigma_k}(x,t)]\Big]dx = 0\end{aligned} \tag{3.28}$$

with some $P_4 > 0$ is added to $\dot V$.

Set $\eta_1 = \mathrm{col}\{z(x,t), z_t(x,t), \varphi(z(x,t)), f_j(x,t), e_j(t)\}$, $j \ne \sigma_k$, and $\eta_2 = \mathrm{col}\{z(x,t), z_t(x,t), \varphi(z(x,t)), f_{\sigma_k}(x,t), e_{\sigma_k}(t)\}$. Then we have

$$\begin{aligned}\dot V(t) + 2\alpha V(t) &\le \sum_{j\ne\sigma_k}^N \textstyle\int_{\Omega_j} \eta_1^T \Psi_1 \eta_1 dx + \int_{\Omega_{\sigma_k}} \eta_2^T \Psi_2 \eta_2 dx \\ &+(2\alpha a_0 P_2 - 2a_0 P_4 + \frac{\lambda_2 l^2}{N^2\pi^2} + \frac{\lambda_3 l^2}{\pi^2}) \int_0^l z_x^2(x,t)dx \\ &+2(\alpha - \varepsilon_1)m(t), \qquad t \in [t_k+\delta, t_k+h_0),\end{aligned}$$

where Ψ_m $(m = 1,2)$ are given by (3.11), (3.12) respectively.

Step 3: For $t \in [t_k+h_0, t_{k+1})$, the ETM is activated. We derive sufficient LMI-based conditions to guarantee that $\dot V(t) + 2\alpha V(t) \le 0$.

From event-triggering condition (2.9), we have

$$\int_{\Omega_{\sigma_k}} [\varepsilon y_{\sigma_k}^2(t) - e_{\sigma_k}^2(t)]dx + \frac{l}{N}\theta m(t) > 0. \tag{3.29}$$

Then, Jensen's inequality implies

$$\lambda_4 \left\{ \textstyle\int_{\Omega_{\sigma_k}} [\varepsilon z^2(x,t) - e_{\sigma_k}^2(t)]dx + \frac{l}{N}\theta m(t) \right\} > 0. \tag{3.30}$$

Differentiating (3.5) along (3.4), we have (3.20), (3.21) and

$$\dot{m}(t)+2\alpha m(t)=(2\alpha-\varepsilon_0)m(t)+\varepsilon y_{\sigma_k}^2(t)-e_{\sigma_k}^2(t). \quad (3.31)$$

Taking (3.19), (3.20)-(3.21), (3.25)-(3.28) and (3.30)-(3.31) into account, we have

$$\begin{aligned}\dot{V}(t)+2\alpha V(t) \le & \sum_{j\neq\sigma_k}^{N} \int_{\Omega_j} \eta_1^T \Psi_3 \eta_1 dx + \int_{\Omega_{\sigma_k}} \eta_2^T \Psi_4 \eta_2 dx \\ & +(2\alpha a_0 P_2 - 2a_0 P_4 + \frac{\lambda_2 l^2}{N^2\pi^2} + \frac{\lambda_3 l^2}{\pi^2}) \int_0^l z_x^2(x,t)dx \\ & +(2\alpha + \tfrac{l}{N}\lambda_4\theta - \varepsilon_0)m(t), \qquad t\in[t_k+h_0, t_{k+1}),\end{aligned}$$

where Ψ_m $(m=3,4)$ are given by (3.13), (3.14) respectively.

Step 4: From Step 1-Step 2, we obtain the feasibility of LMIs (3.7)-(3.9) implies that any strong solution of (2.12), (2.3) initialized with z_0 admits a priori estimate

- $V(t) \le e^{2\alpha_0(t-t_k)}V(t_k)$, $\forall t\in[t_k, t_k+\delta)$,
- $V(t) \le e^{-2\alpha(t-t_k-\delta)}V(t_k+\delta)$, $\forall t\in[t_k+\delta, t_{k+1})$.

Since $\alpha_1<\alpha$ and $t_{k+1}-t_k\ge h_0$, (3.15) implies

$$(\alpha_1-\alpha)(t_{k+1}-t_k) \le (\alpha_1-\alpha)h_0 \le -(\alpha_0+\alpha)\delta. \quad (3.32)$$

If $0<\alpha_1 h_0 \le \alpha h_0 - (\alpha_0+\alpha)\delta$, one has

$$V(t_{k+1}) \le e^{2\alpha_0\delta-2\alpha(t_{k+1}-t_k-\delta)}V(t_k) \le e^{-2\alpha_1(t_{k+1}-t_k)}V(t_k), \ .$$

For $t\in[t_k, t_k+\delta)$, $V(t)\le e^{2\alpha_0\delta}V(t_k)$. For $t\in[t_k+\delta, t_{k+1})$, $V(t)\le V(t_k+\delta)\le e^{2\alpha_0\delta}V(t_k)$. Therefore, we have

$$\begin{aligned} V(t) &\le e^{2\alpha_0\delta}V(t_k) \le e^{2\alpha_0\delta-2\alpha_1(t_k-t_{k-1})}V(t_{k-1}) \\ &\le \cdots \le e^{2\alpha_0\delta-2\alpha_1 t_k}V(0), \ t\in[t_k, t_{k+1}).\end{aligned}$$

The latter bound for $t_k=0$ guarantees the existence of the strong solutions for all $t\in[0,t_1]$. Then using step method [26], we conclude that the strong solution exists for all $t\ge 0$. Moreover, the closed-loop system is asmyptotically stable. ■

Under the Neumann boundary conditions, the result is similar:

Theorem 3.2: Consider the closed-loop system (3.4) subject to Neumann boundary conditions (2.3). Given positive parameters K, h_0, θ, ε_0, ε, α, δ, $\varepsilon_1>\alpha$, $h_0>\delta$ and tuning parameter α_0 such that $\alpha h_0 > (\alpha_0+\alpha)\delta$, let there exist scalars $P_n\ge 0$ $(n=1,2,3,4)$, $\lambda_i\ge 0$ $(i=0,1,2,4)$ and $R\ge 0$ that satisfy the LMIs (3.7)-(3.9) with $\lambda_3=0$. Let α_1 be subject to (3.15). Then the closed-loop system (2.12) subject to (2.3) and (2.7) is asymptotically stable for any initial function $z_0\in H_0^1(0,l)$.

Remark 3.1: Note that the Wirtinger's inequality becomes invalid for the case of the Neumann boundary condition. Therefore, Inequality (3.27) cannot be applied. The system (2.1) under the Neumann boundary conditions is exponentially stable if the LMI conditions of Theorem 3.1 hold with $\lambda_3=0$.

Remark 3.2: Inspired by the switching (time-triggered) controllers (see our previous works [18], [25]), according to the Lyapunov function (3.5), the maximal value of h_0 can be calculated by LMIs $\Psi_l<0, (l=0,1,2)$. In this paper, our switching-based event-triggered controller leads to larger inter-execution times in average than the switching (time-triggered) controller in the example below.

IV. Numerical Illustration

In the following, a numerical example is provided to verify the effectiveness of the proposed method. Consider nonlinear reaction-diffusion equation (2.1) under the Dirichlet boundary conditions (2.3) with $l=1$ and $a(x)=a_0=1$. The initial condition and the nonlinear function are chosen as $z(x,0)=z_0(x)=2\sin(\pi x)(1-\cos(\pi x))$ and $\varphi(z(x,t))=(1-\exp(-5z^2(x,t)))$ respectively. As clearly visible in Fig. 1(a), the open-loop system is unstable.

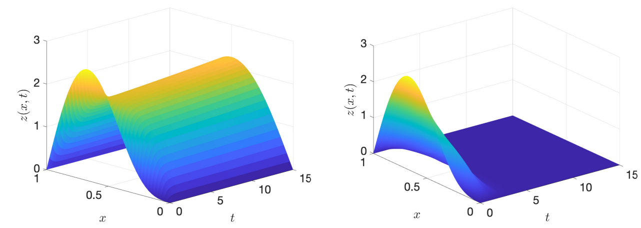

(a) (b)

Fig. 1. (a) State of unforced system; (b) State of closed-loop system

To verify the LMI conditions of Theorem 3.1, some parameters of the controlled system (3.4) and dynamic ETM (2.9) are chosen as follows:

$$\begin{aligned}&\theta=1, \quad \varepsilon=0.4, \quad \varepsilon_0=2.5, \quad N=10, \ K=3, \\ &\alpha=0.07, \ \alpha_0=1.1, \ \alpha_1=0.01, \ h_0=0.1, \delta=0.005.\end{aligned}$$

Then by Yalmip, the following feasible solutions of LMIs are obtained:

$$\begin{aligned}&P_1=4.2625, \quad P_2=1.8358, \quad P_3=7.3898, \ P_4=1.6756, \\ &R=2.9907, \quad \lambda_0=13.1494, \ \lambda_1=1.7048, \ \lambda_2=25.0164, \\ &\lambda_3=24.4262, \ \lambda_4=9.0144.\end{aligned}$$

Set the steps in time and space as $dx=0.01$ and $dt=10^{-4}$, respectively. A finite difference method is utilized to compute the numerical solution of the closed-loop system (2.12) subject to (2.3) under the switching-based event-triggered control law

$$u_{\sigma_k(t)}=\begin{cases} 0, & t\in[t_k, t_k+0.005), \\ -3\int_{\Omega_{\sigma_k}} z(x,t_k)dx, & t\in[t_k+0.005, t_{k+1}) \end{cases}$$

via the switching rule (2.7) and ETM (2.9). The behavior of the closed-loop system is presented in Fig. 1(b). As expected, the resulting closed-loop system is exponentially stable.

Furthermore, the trajectories of $e_{\sigma_k}(t)$ are visualized in Fig. 2(a). Fig. 2(b) shows that the release time and release interval under dynamic ETM for $t\in[0,15]$. The switching-based event-triggered controllers are depicted in Fig. 2(c). The locations of actuator are given in Fig. 2(d). These simulation results confirm the theoretical results.

Table I shows the amount of sent measurements and the maximal values of h_0 with different values of ε, θ and m_0 in dynamic ETM (2.9). From the simulation results, we find that the sent measurements are reduced by choosing larger ε, θ and m_0. The maximal value of h_0 is decreased with a larger ε. The last line in Table I (with $\varepsilon=\varepsilon_0=\varepsilon_1=\theta=0$) corresponds to time-triggered switching control (considered

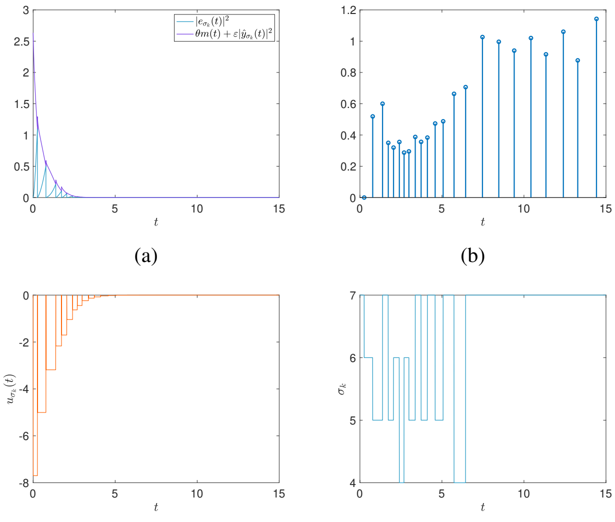

(a) (b) (c) (d)

Fig. 2. (a) Trajectories involved in the dynamic ETM (2.9); (b) Release instants and release interval by dynamic ETM (2.9); (c) Switching-based event-triggered controller; (d) Actuator locations for $N = 10$

TABLE I

COMPARISON WITH DIFFERENT VALUES OF ε, θ AND m_0

ε	θ	m_0	Sent measurements	Maximal value of h_0
0.4	0.2	0	27	0.3244
0.4	0.5	0	25	0.3244
0.4	1	0	23	0.3244
0.4	1	5	21	0.3244
0.4	1	10	20	0.3244
0.8	1	10	18	0.3227
1.4	1	10	17	0.3177
0	0	0	45	0.3306

in our previous works [18], [25]). It is seen that the suggested ETM reduces the number of sent measurements (17 compared with 45) at least by 2.5 times.

V. CONCLUSIONS

The present paper discusses a dynamic switching-based event-triggered control design to stabilize a reaction-diffusion equation by output-dependent switching. The well-posedness and exponential stability analysis of the system has been estabilished. One of the directions for the future research is extension of the obtained results to high-dimensional PDE systems.

REFERENCES

[1] Girard, A. (2015). Dynamic triggering mechanisms for event-triggered control. *IEEE Transactions Automatic Control*, 60(7), pp. 1992-1997.
[2] Tabuada, P. (2007). Event-triggered real-time scheduling of stabilizing control tasks. *IEEE Transactions Automatic Control*, 52(9), pp. 1680-1685.
[3] Heemels, W., Donkers, M. (2013). Model-based periodic event-triggered control for linear systems. *Automatica*, 49(3), pp. 698-711.
[4] Rthnayake B, Diagne M, Espitia N, Karafyllis I. (2022). Observer-based event-triggered boundary control of a class of reaction-diffusion PDEs. *IEEE Transactions Automatic Control*, 7(6), pp. 2905-2917.
[5] Kang, W., Baudouin, L., Fridman, E. (2021). Event-triggered control of Korteweg–de Vries equation under averaged measurements. *Automatica*, 123, pp. 109315.
[6] Selivanov, A., Fridman, E. (2016). Distributed event-triggered control of diffusion semilinear PDEs. *Automatica*, 68, pp. 344-351.
[7] Davó, M., Bresch-Pietri, D., Prieur, C., and Di Meglio, F. (2019). Stability analysis of a 2×2 linear hyperbolic system with a sampled-data controller via backstepping method and looped-functionals. *IEEE Transactions on Automatic Control*, 64(4), pp.1718-1725.
[8] Espitia, N., Yu, H., Krstic, M. (2020). Event-triggered varying speed limit control of stop-and-go traffic. *IFAC-PapersOnLine*, 53(2), pp. 7509-7514.
[9] Espitia, N., Karafyllis, I., Krstic, M. (2021). Event-triggered boundary control of constant-parameter reaction-diffusion PDEs: A small-gain approach. *Automatica*, 128, pp. 109562.
[10] Selivanov, A., Fridman, E. (2016). Event-triggered H_∞ control: a switching approach. *IEEE Transactions on Automatic Control*, 61 (10), pp. 3221-3226.
[11] Huang Y, Liu Y. (2019). Switching event-triggered control for a class of uncertain nonlinear systems. *Automatica*, 108, pp.108471.
[12] Su, X., Liu, X., Shi, P., Song, YD. (2018). Sliding mode control of hybrid switched systems via an event-triggered mechanism. *Automatica*, 90, pp. 294-303.
[13] Katz, R., Fridman, E., Selivanov, A. (2021). Boundary delayed observer-controller design for reaction-diffusion systems, *IEEE Transactions on Automatic Control*, 66(1), pp. 275-282.
[14] Iftime, O.V., Demetriou, M.A. (2009). Optimal control of switched distributed parameter systems with spatially scheduled actuators. *Automatica*, 45, pp. 312-323.
[15] Zuazua, E. (2010). Switching control. *Journal of the European Mathematical Society*, 13, pp. 85-117.
[16] Wu, H.N., Zhang, X.W. (2019). Integrated design of switching control and mobile actuator/sensor guidance for a linear diffusion process. *Journal of the Franklin Institute*, 356, pp. 7246-7262.
[17] Wu, H.N., Zhang, X.W. (2020). Static output feedback stabilization for a linear parabolic PDE system with time-varying delay via mobile collocated actuator/sensor pairs. *Automatica*, 117, pp. 108993.
[18] Kang, W., Fridman, E., Liu, C.X. (2023). Stabilization by switching of parabolic PDEs with spatially scheduled actuators and sensors, *Automatica*, 147, pp. 110668.
[19] Mu, W., Qiu, F., Zhuang, B., Chen, L. (2021). Optimal actuator switching synthesis of observer-based event-triggered state feedback control for distributed parameter systems, Journal of the Franklin Institute, 358(1), pp. 384-399.
[20] Jiang, Z., Cui, B., Wu, W., Zhuang, B. (2016). Event-driven observer-based control for distributed parameter systems using mobile sensor and actuator, Computers & Mathematics with Applications, 72(12), pp. 2854-2864.
[21] Wen, Y., Lou, X., Chen, J., Chen, Y. (2022). Mobile Actuator-Plus-Sensor Strategy for Event-Driven Observer-Based Control of Delayed Distributed Parameter Systems, IEEE Control Systems Letters, 6, pp. 2162-2167.
[22] Jiang, Z., Zhuang, B., Lou, X., Wu, W. (2022). Integrated Design of Event-triggered Control and Mobile Non-collocated SANs for a Diffusion Process. *International Journal of Control, Automation and Systems*, 20(9), pp. 2915-2926.
[23] Fridman, E., Bar Am, N. (2013). Sampled-Data Distributed H_∞ Control of Transport Reaction Systems. *SIAM J. Control & Optimization*, 51(2), pp. 1500-1527.
[24] Fridman, E., Blighovsky, A. (2012). Robust Sampled-Data Control of a Class of Semilinear Parabolic Systems. *Automatica*, 48, pp. 826-836.
[25] Kang, W., Fridman, E., Liu, C.X. (2021). Stabilization for a semilinear heat equation with switching control, *2021 60th IEEE Conference on Decision and Control (CDC)*, pp. 448-453.
[26] Fridman, E. (2014). *Introduction to Time-Delay Systems: Analysis and Control*. Basel: Birkhäuser.
[27] Henry, D. (1981). *Geometric theory of semilinear parabolic equations*. New York: Springer-Verlag.